Radiation-Assisted Morphology Modification of LDPE/TPS Blends: A Study on Starch Degradation-Processing-Morphology Correlation

K. A. Dubey,[1] C. V. Chaudhari,[1] Naina Raje,[2] Lata Panickar,[3] Y. K. Bhardwaj,[1] S. Sabharwal[1]

[1]*Radiation Technology Development Division, Bhabha Atomic Research Centre, Trombay, Mumbai 400085, India*
[2]*Analytical Chemistry Division, Bhabha Atomic Research Centre, Trombay, Mumbai 400085, India*
[3]*Solid State Physics Division, Bhabha Atomic Research Centre, Trombay, Mumbai 400085, India*

Received 19 May 2011; accepted 12 August 2011
DOI 10.1002/app.35466
Published online 21 November 2011 in Wiley Online Library (wileyonlinelibrary.com).

ABSTRACT: Potato starch was radiolytically degraded to different extents by irradiating with Co-60 gamma radiation in wide dose range. The degraded starch was plasticized using glycerol and water to obtain radiation processed thermoplastic starch (RTPS). Blends of different RTPS and low density polyethylene (LDPE) were prepared by internal melt mixing. Characterization of blends using differential scanning calorimetry, thermogravimetric analysis, X-ray diffraction, Fourier transformed infrared spectroscopy, scanning electron microscope, melt flow, contact angle, and soil burial studies indicated changes in the blend morphology and biodegradation behavior with the increase in the dose imparted to the starch fraction. Molecular weight of starch decreased substantially in the dose range of the study. The melt viscosity of LDPE/RTPS blend decreased whereas crystallinity of LDPE phase increased with the incorporation of RTPS. No significant change in the carbonyl index and thermal stability of the blends was observed in the dose range studied; therefore, the observed changes in the physical and thermal properties of the blends were attributed primarily to the kinetic factors affecting crystallization and time-dependent phase separation process. Biodegradability of blends varied with the radiation dose imparted to starch component of blend, suggesting better encapsulation of RTPS by LDPE chains.
 J Appl Polym Sci 124: 3501–3510, 2012

Key words: radiation; thermoplastic starch; blends; biodegradable polymers

INTRODUCTION

Development of partially or fully biodegradable polymer material having good physico-mechanical properties, desired biodegradation behavior, and low cost has been a challenge to the present date.[1–4] This is mainly due to unavailability of a natural metabolism route for synthetic polymers and the inherent incompatibility of natural and synthetic polymers. Polyolefin/natural polymer blends have gained considerable interest in this regards, as these blends are expected to be partially biodegradable and cost effective.[5,6] Moreover, microbial consumption of the natural polymer component in polyolefin/natural polymer blends is expected to show increased porosity, void formation, and the loss of integrity of the polyolefin phase, eventually increasing the rate of oxidative degradation of polyolefin.[6]

Starch is easily metabolized by a wide range of microorganisms and unlike other natural polymers can be processed as a thermoplastic material after suitable plasticization. Low density polyethylene (LDPE) is a versatile polymer for various applications because of its relatively low cost, easy availability, and good processability. In recent years, blending of thermoplastic starch (TPS) with LDPE has gained considerable importance for enhancing biodegradation of LDPE at an acceptable cost without many inputs in LDPE processing technology.[7–9] However, on blending TPS with LDPE, processability and mechanical properties of LDPE deteriorate significantly due to poor interfacial compatibility.[5–8,10] Such drawbacks, to some extent are expected to be overcome using high energy radiation for blend modification, as high energy radiation can be effectively used to modify the interface and bulk properties of polymers.[11–18] Solvation and other chemical reaction of cellulosic polymers have been reported to be less energy and chemical intensive with the use of ionizing radiations.[19,20] In addition, high energy radiation can be used to reduce or increase the molecular weight of polymeric material. The low operation cost, additive free technique, and room temperature operations are among the added advantages of radiation technology over other techniques.[21,22]

This article reports the use of high energy radiation to modify chain length and microstructure of starch. Blends of LDPE and radiation processed

Correspondence to: Y. K. Bhardwaj (ykbhard@barc.gov.in).

thermoplastic starch (RTPS) containing different extent of radiolytically degraded starch have been prepared and characterized. The changes in the morphological, crystallographic, and spectroscopic characteristics of LDPE/TPS blends on introduction of RTPS are presented here. Efforts have also been made to establish morphology–property correlation using differential scanning calorimetry (DSC), thermo gravimetric analysis (TGA), X-ray diffraction (XRD), Fourier transformed infrared (FTIR) spectroscopy, melt flow, scanning electron microscope (SEM), contact angle, and soil burial studies.

EXPERIMENTAL AND METHODS

Materials

LDPE in form of pellets (trade name Indothene) from local supplier M/s HPCL, Mumbai, India, was used as received. The potato starch and glycerol (purity >98%) were procured from S. D. Fine chemicals, India. Specifications of the polymers used in the study are mentioned in Table I. Freshly prepared double distilled water was used for synthesis of TPS and water uptake studies.

TABLE I
Sample Designations of LDPE/RTPS Blends

LDPE (%)	TPS (%)	Dose imparted to starch (kGy)	Designation
70	30	00	LT_0
70	30	5	LT_5
70	30	10	LT_{10}
70	30	25	LT_{25}
70	30	50	LT_{50}

LDPE: specific gravity: 0.93; Melting point: 103 °C. Starch: Source: potato (Insoluble); amylose 19%; amylopectin 81%; moisture content 9.19% (by weight).

Methods

Sample preparation

Starch samples were irradiated to different radiation doses in the dose range 5–50 kGy and then plasticized with glycerol (25%) and water (5%) at 100°C to prepare TPS.[16,18,23] Blends of TPS (made from irradiated and unirradiated starch) and LDPE (70 : 30) were prepared by mixing components in Brabender plasticorder. The homogeneously mixed samples so formed were cut into small pieces, and compressed into sheets of size 12×12 cm^2 of different thicknesses in range 0.2–1 mm using compression-molding machine at 150 kg/cm^2 pressure for 2 min at 130°C. Sample compositions and their designations have been presented in Table I.

Irradiation

Irradiation was performed under aerated condition in gamma chamber 5000 (GC-5000) having Co-60 gamma source supplied by M/s BRIT, India. The dose rate of gamma chamber was ascertained to be 2.5 kGy h^{-1} by Fricke dosimetry before irradiation of samples. The starch samples in powder form were initially dried at 60°C for 24 h and later irradiated under sealed conditions.

FTIR studies

FTIR spectroscopy measurements were performed using spectrophotometer (JASCO, model FT/IR-610) in attenuated total reflectance (ATR) mode for ascertaining composition of the blends. The samples were neatly pressed inside the sample holders, and the spectra recorded in the range 400–4000 cm^{-1} with a resolution of 4 cm^{-1} and averaged over 100 scans.

Molecular weight determination

The molecular weight of starch was determined by dilute solution viscometry (DSV). All measurements were performed at 25°C using dilution Ubbelholde type capillary viscometer immersed in a constant temperature bath. The stock solutions (0.5 g dL^{-1}) of starch irradiated to different doses were made in 1 *M* NaOH. Dilutions to yield at least six lower concentrations were made by adding appropriate aliquots of solvent (1 *M* NaOH). The solutions were filtered through sintered glass filter before DSV studies. The elution time of each solution was determined as average of several readings. From the intrinsic viscosity, the molecular weight of the starch was determined using Mark–Houwink equation ($[\eta] = kM^{\alpha}$, where $[\eta]$ is the intrinsic viscosity, M is the molecular weight, k and α are Mark–Houwink parameters). The values of k and α for the system were taken as 8.36×10^5 and 0.77, respectively.[24]

Melt flow index measurements

Melt flow index (MFI) was determined as per ASTM D2839-05 standard, using MFI tester supplied by M/s International Equipments, Mumbai.

Water uptake studies

The prepared samples were dried under vacuum for 24 h. The dried blends so obtained were cut into uniform circular pieces 1 cm diameter using a sharp edged die and used for water uptake studies. Preweighed samples were placed in a 200-mesh stainless steel compartment and immersed in excess water at 30°C. The swelled samples were periodically removed, blotted free of surface water using laboratory tissue paper, weighed on AND analytical balance

(accuracy 0.00001 g) in stopper bottles, and returned to the swelling medium. Measurements were taken until the samples reached constant weight.

Differential scanning calorimetry

Differential scanning calorimetry (DSC-822 from M/s Mettler) of blends was performed to estimate change in crystallinity of the blends. All specimens were initially scanned from 0 to 150°C at 5°C min^{-1}, cooled back at 20°C to room temperature and rescanned at 5°C min^{-1} to 130°C. Heat capacity thermograms for the second run have been reported. All thermograms were recorded, under inert argon atmosphere. Before DSC run the instrument that was calibrated for temperature and heat flow using high purity indium standard. The crystallinity of the blends was estimated using relation below

$$X_c(\%) = \Delta H/\Delta H^{\circ} \times 100 \quad (1)$$

where ΔH and ΔH° are the melting enthalpies of the sample and 100% crystallized sample, respectively. ΔH was acquired by the integral area of a DSC heating curve associated with melting event in DSC curve and ΔH° for LDPE (100% crystalline) was assumed 279 J/g.[25,26] ΔH were normalized to respective polymer components.

Thermogravimetric analysis

Thermal stability of the samples was investigated by recording the thermogravimetric (TG) patterns in the temperature range of RT-600°C under N_2 atmosphere at a heating rate of 10°C/min using Netzsch thermal analyzer [Model: STA 409 personal computer (PC) LUXX] 100 mL/min. Carrier gas flow rate was used for all the measurements. Alumina crucibles were used as sample/reference holder.

Morphological studies

Cryogenically fractured surfaces were examined by SEM. Acceleration voltages of 30 kV and magnification range from 200 × to 5000 × were used. The fractured surfaces were coated with a thin layer of gold before SEM examination.

X-ray diffraction studies

XRD patterns were recorded using a Philips X-ray diffractometer PW 1710 (Almelo, Netherlands) using monochromatized CuK_{α} radiation from an X-ray generator operated at 30 kV and 20 mA.

Wettability and surface energy analysis

The measurement of contact angles of the sample was performed by sessile drop technique using image analysis software. A liquid droplet (1.5–2.5 μL) was allowed to fall on the samples to be studied from a software-controlled syringe. An image sequence was taken through a charge-couple device (CCD) camera of goniometer from GBX instruments, France that was connected to a PC computer and interfaced to image capture software (Windrop^{++}, GBX instruments).

Owens and Wendt method was used to determine the total surface energy and its resolution into polar and dispersive component, wherein the total solid surface tension γ was assumed to be of the general form[27]

$$1 + \cos\theta = 2\sqrt{\gamma_s^d}\left(\sqrt{\gamma_1^d}/\gamma_1\right) + 2\sqrt{\gamma_s^p}\left(\sqrt{\gamma_1^p}/\gamma_1\right) \quad (2)$$

In this equation, the subscripts s and 1 refer to the solid and liquid surface tension, respectively; the superscripts d and p coincide with dispersive and polar components of total surface tension, where sum of these two values are equal to the total surface tension. The $\sqrt{\gamma_s^d}$ and $\sqrt{\gamma_s^p}$ are needed to be resolved. Therefore, two independent contact angles were measured by two different liquids water and diiodomethane. γ_1, γ_1^d, and γ_1^p were experimentally determined to be 68.9, 18.6, and 50.3 mN/m for water and 49.7, 48.0, and 1.7 mN/m for diiodomethane.

Soil burial studies

The biodegradation behavior of the blends was investigated by soil burial testing under natural flora and fauna conditions. Samples ~ 200 μm thick of size 5 × 3 cm^2 were placed under soil at a depth of 20 cm in properly marked plastic mesh trays, to allow access of microorganism and moisture. The plastic mesh allowed safe retrieval of samples after 3 months. After removal, samples were thoroughly washed with tap water finally with distilled water and dried at 60°C in a vacuum oven for 24 h. Weight difference (before and after burial) was determined gravimetrically.

RESULTS AND DISCUSSION

Effect of radiation dose on the melt processing parameters

Thermal processing of starch-based polymers is more difficult than processing of synthetic polymers due to associated entanglements and secondary bonding structure. Native starch is semicrystalline due to the intramolecular and intermolecular hydrogen bonding between the hydroxyl groups. Processing of starch using Brabender/mixer has been reported to disrupt intermolecular and intramolecular hydrogen bonding

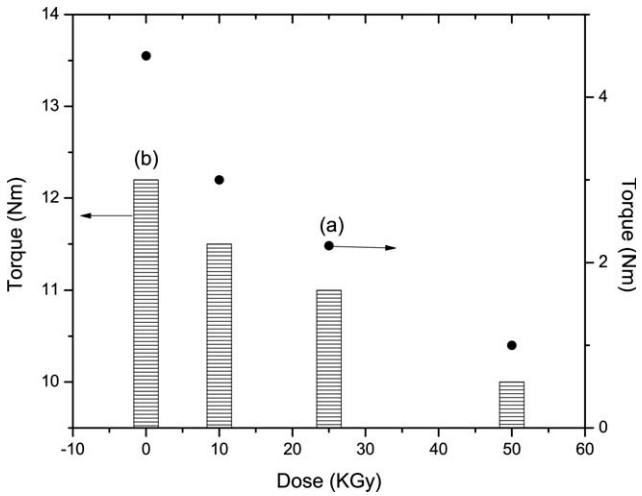

Figure 1 Torque values derived from Brabender profiles at 30 rpm, 100°C after 10 min for (a) TPS prepared from starch irradiated to different doses and (b) blending of LDPE and RTPS.

to form a homogeneous amorphous material.[10,28,29] Thus, studies on variation of torque with time and temperature in Brabender can provide an insight into the gelatinization process and rheological properties of starch under shear stress conditions.[17] Figure 1 shows torque generated during processing of TPS irradiated to different doses, and LDPE/RTPS blends containing starch irradiated to different doses in Brabender at 30 rpm, 100°C after 10 min. It is clear that with increase in absorbed radiation dose for TPS, torque reduces substantially from 4.5 Nm to 1 Nm, which can be attributed to the lowering in the melt viscosity of TPS due to radiolytic degradation of starch. Reduction in torque was also observed during blending of LDPE and RTPS, however, reduction in torque (12.2 Nm–10 Nm) was not as substantial as during processing of starch. This can be understood considering the fact that reduction in the torque is mainly due to the reduction in the molecular weight of starch. As only 30% (w/w) TPS was used in the blends, torque of the system was expected to be less susceptible to variations in the molecular weight of the starch.

Effect of irradiation on molecular weight of starch and MFI

The variation in molecular weight of starch with absorbed radiation dose has been presented in Figure 2. The molecular weight of starch decreased sharply upto 25 kGy followed by slower reduction at higher doses indicating predominantly radiation induced degradation of starch on irradiation. Similar molecular weight reduction to different extents on irradiation of starch of different origin has been reported earlier.[14] Figure 2 also shows the effect of addition of RTPS on MFI of LDPE matrix. MFI of LDPE/RTPS blend was higher than that of LDPE/TPS blend and it showed a sustained increase with increase in the radiation dose. This suggests higher mobility of polymer chains of blends in the presence of RTPS. This again can be explained on the basis of the discussion provided in earlier sections, that is, with increase in the radiation dose; molecular weight of starch decreases, resulting in less hindrance from starch to diffusion of LDPE polymer chains.[30,31] As MFI can be correlated to material viscosity, these results also indicated that LDPE/RTPS had a lower viscosity than LDPE/TPS.

FTIR analysis of LDPE/RTPS blends

The FTIR spectra of different LDPE/RTPS blends were recorded. All samples exhibited characteristic peaks of starch and LDPE.[32–35] The band in region 3000–3600 cm^{-1} (O—H stretching), 2900–3000 cm^{-1} (C—H stretching), 1150, 1124, and 1103 cm^{-1} (C—O, C—C stretching with some C—OH contributions), 1077, 1047, 1022, 994, and 928 cm^{-1} (C—OH bending and CH_2 elated modes), and 861 cm^{-1} (COC symmetrical stretching and CH deformation) were attributed to starch. The characteristic symmetrical and asymmetrical stretching of ethylene segments were observed at 2915 cm^{-1} and 2846 cm^{-1}. The peaks observed at 1475 cm^{-1}, 1368 cm^{-1}, and 718 cm^{-1} were attributed to deformation vibration of methylene, flexural vibration of methyl, and inner rocking vibration of methylene, respectively. It has been reported that gamma irradiation degrades and oxidizes starch, and thereby can affect the interaction between LDPE and TPS chains.[34] An attempt was made to use FTIR to monitor such interactions. The transmittance observed in the hydroxyl region was found to have an asymmetrical shape and peak shifts with introduction of irradiated starch (Table II). Changes observed in transmittance of this band can be attributed to changes in the molecular

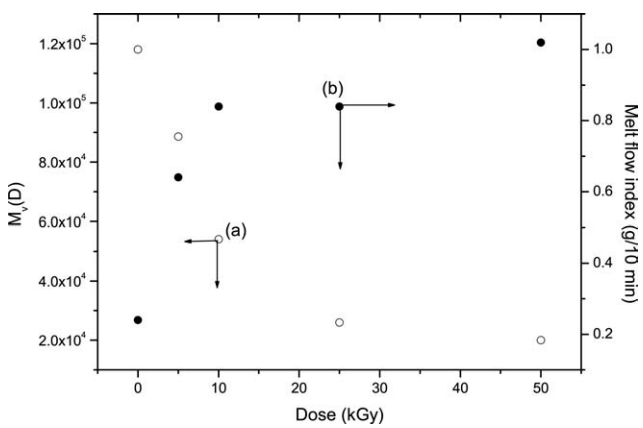

Figure 2 Effect of irradiation on (a) change in the molecular weight and (b) MFI of LDPE/RTPS.

TABLE II
Observed Main Peaks of LDPE and RTPS in FTIR Spectra and their Assignments

Blend	—OH (cm^{-1})	Bound water (cm^{-1})	Starch (amorphous) (cm^{-1})
LT_0	3361	1638	1461
LT_5	3367	1641	1461
LT_{10}	3391	1633	1462
LT_{25}	3346	1633	1462
LT_{50}	3346	1633	1462

environment of the primary hydroxyl group in amylose, mainly due to changes in intramolecular hydrogen bonding. However, it was not possible to assign the bands unambiguously because most bands resulted from highly coupled vibrational spectra bands into poorly resolved bands in the spectrum. A slight yellowing of starch after radiation treatment was observed because of its radiolytic oxidation. No prominent peak in the carbonyl region was observed. However, some evidence of carbonyl group in form of a shoulder to bound water peak at 1640 cm^{-1} was there. It may also be noted that no major peak at 947 cm^{-1}, assigned to conformation change[36] was observed, suggesting amylopectin conformation largely remains unchanged on irradiation and blending.

Thermal behavior of LDPE/TPS blends

Figure 3 depicts crystallization and melting thermograms of LDPE/TPS blends. The crystallinity (X_c), melting (T_m), and crystallization (T_c) temperatures are shown in Table III. The crystallization temperature of LDPE shifts from 92.3°C in neat state to 93.9°C in the blends. The shift of T_c to higher temperature is indicative of increase of LDPE's crystallization rate on the incorporation of irradiated TPS, as the blend system is noninteractive (see "Effect of irradiation on molecular weight of starch and melt flow index" Section). Crystallinity of LDPE also increased substantially on using irradiated starch. The result suggests the disruption in the crystallization of LDPE phase due to intrusion and intermingling of starch chains reduced when starch irradiated to higher dose was used. Similar increase in crystallinity of parent matrix in the presence of fillers has been reported earlier for other systems.[37] This observation can be understood in view of the fact that starch being predominantly, degrading type of polymer, will undergo substantial chain scission after irradiation, and the low molecular weight starch produced on radiation degradation may not show as crystallization inhibitory effect as shown by unirradiated starch of comparatively high molecular weight. The decrease in melting temperature with use of irradiated starch, on the other hand, suggested the low thermodynamic stability of LDPE crystallites. Such a low stability of LDPE crystallites in RTPS blends may be attributed to the wider molecular weight distribution of irradiated starch, which though increases the crystalline content of LDPE but results in imperfect crystallization. It may also be noted that maximum change in the crystallinity was observed at high doses (LT_{50}), suggesting a critical radiation dose might be necessary to observe such a phenomenon.

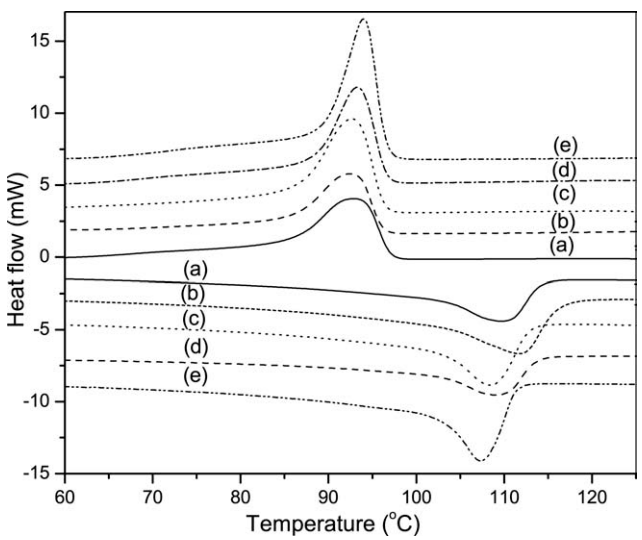

Figure 3 Crystallization and melting thermograms of (a) LT_0, (b) LT_5, (c) LT_{10}, (d) LT_{25}, and (e) LT_{50}.

TABLE III
DSC Parameters for LDPE/RTPS Blends

Blends	Crystallinity (%)	T_m (°C)	T_c (°C)
LT_0	34.17	109.7	92.3
LT_5	34.60	109.4	92.3
LT_{10}	35.10	108.4	92.7
LT_{25}	35. 48	108.1	93.1
LT_{50}	39.40	107.4	93.9

The TG curves of different LDPE/RTPS blends and of pure LDPE are shown in Figure 4. As shown in Figure 4, LDPE displayed single step degradation process (a single peak around 480°C in DTGA profile). The LDPE/RTPS blends, however, showed a complex profiles with four degradation steps and three distinct peaks at around 100, 308, and 480°C on DTG curve, which were attributed to decomposition of starch and LDPE domains, respectively.[38] The peak as well as step due to glycerol was found to be very broad and appeared as a shoulder to the starch peak. At the end of all runs, black residue was seen which may due to starch component of blends though it has been reported that the residue does not have any quantitative relation with the starch present in the matrix.[39] The DTG peak

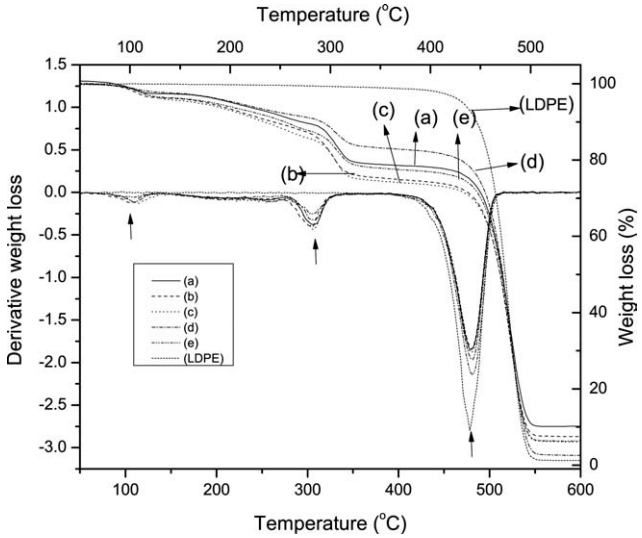

Figure 4 Thermogravimetric profiles of (a) LT_0, (b) LT_5, (c) LT_{10}, (d) LT_{25}, and (e) LT_{50}: (A) TGA and (B) DTGA.

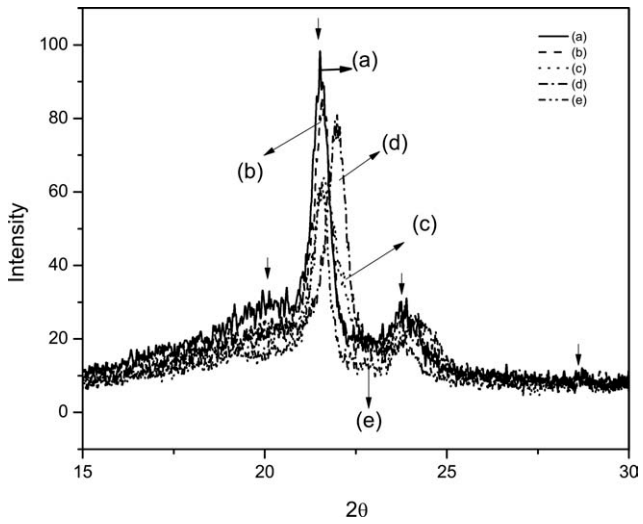

Figure 5 X-ray diffractograms of (a) LT_0, (b) LT_5, (c) LT_{10}, (d) LT_{25}, and (e) LT_{50}.

temperatures of all the blends are shown in Table IV. It is clear from the table that thermal stability of the blends is largely unaffected by radiation. This finding highlights the fact that the interaction between starch and LDPE is not significant enough to affect the thermal stability of each other. It also indicates that degradation induced by high energy radiation does not adversely affect the thermal degradation stability of the starch in the dose range of this study.

X-ray diffraction studies of LDPE/TPS blends

The X-ray diffractograms of all the blends were recorded to ascertain crystallinity behavior of the samples and to determine changes in the crystallographic parameters. The X-ray diffractograms of the blends are shown in Figure 5. All samples showed three crystalline peaks at 21, 23, and 35.6° that were attributed to (110), (200), and (020) characteristic crystal planes of LDPE, respectively.[40] Crystalline component of starch is expected to show a peak at 13.5°; however, no such peak was observed in any of the samples. This observation suggests complete destruction of crystallinity of starch during plasticization and blend formation processes. The incorporation of RTPS into LDPE did not affect the crystalline structure of LDPE, as the blend also exhibited an orthorhombic structure typical of LDPE and no significant shift in the peak position was observed. Lattice constant and lateral crystal size were calculated for the (110) and (200) planes for all the samples.[41] The Bragg equation [Eq. (3)] was used to calculate the lattice distance ($d_{h\ k\ l}$)

$$d_{hkl} = \frac{\lambda}{2 \sin \theta_{hkl}} \tag{3}$$

where λ is 1.541A and $\theta_{h\ k\ l}$ represents Bragg angle. The lateral crystal size $l_{h\ k\ l}$ was calculated by Scherrer formula given by

$$l_{hkl} = \frac{\beta\lambda}{f_{hkl} \cos \theta_{hkl}} \tag{4}$$

where the structure factor β is taken as 1 and $f_{h\ k\ l}$ is the full width at half maxima of the crystal plane reflection.[42] The crystallinity of the samples was obtained from the peak area analysis by WAXD. The ratio of the area under the crystalline peaks to the entire area under the diffraction curve represents the crystallinity. The overall crystallinity X_c was calculated using equation

$$X_c = \frac{\sum I_c}{\sum I_c + \sum I_a} \tag{5}$$

where I_c and I_a are the fitted crystalline and amorphous areas, respectively. The results of studies are given in Table V. From the table it can be seen that the crystallinity and lattice parameters changed on

TABLE IV
TGA Parameters for LDPE/RTPS Blends

Sample	Peak degradation temperature of starch (°C)	Peak degradation temperature of LDPE (°C)	LDPE (%)
LT_0	305.6	478.1	67
LT_5	305.6	478.1	66
LT_{10}	305.6	478.1	66
LT_{25}	305.6	478.1	69
LT_{50}	305.6	478.1	67
LDPE	NA	478.1	99

TABLE V
Crystallographic Parameters for LDPE/RTPS Blends

Sample	X_c (%)	$\theta_{1\,1\,0}$ (°)	$\theta_{2\,0\,0}$ (°)	$d_{1\,1\,0}$ (Å)	$l_{1\,1\,0}$ (Å)	$d_{2\,0\,0}$(Å)	$l_{2\,0\,0}$(Å)
LT_0	31.73	10.76	11.91	4.12	199.37	3.73	165.08
LT_5	31.83	10.79	11.95	4.11	185.22	3.72	165.94
LT_{10}	33.15	10.83	12.02	4.10	183.75	3.69	153.39
LT_{25}	34.55	10.77	11.94	4.12	191.19	3.72	138.53
LT_{50}	37.18	10.98	12.13	4.04	164.31	3.66	137.06

incorporation of RTPS in the LDPE. Crystallinity increased with radiation dose. Although there was not much lattice shift, however, lateral crystal size decreased substantially for irradiated starch samples. These results support DSC studies, wherein increase in crystallinity was observed with reduction in crystallite dimensions indicating imperfect crystallization which might reflect as decrease in the melting point.[43] It may be noted that though a conclusive remark on the crystallite size cannot be made without a detailed investigation of crystal growth dynamics, however, considering DSC and XRD results and SEM analysis discussed in the next section, it can be safely concluded that RTPS does affect the morphology and crystallization pattern of LDPE.

Morphology of LDPE/TPS blends

Scanning electron micrographs of fractured blend surfaces have been shown in Figure 6. SEM of LDPE/TPS blend (LT_0) showed substantial phase separation, whereas LT_{50} matrix was uniform. It can be seen from the figures, there is a gradual improvement in the blend morphology. For samples LT_0 to LT_{25}, LDPE clearly exists as continuous phase with TPS as dispersed phase whereas LT_{50} was relatively homogeneous. From SEM studies it is difficult to draw a quantitative estimate due to asymmetric shapes and distribution of starch granules. The variation in the dispersion pattern of TPS in LDPE with the use of RTPS can be attributed to lower molecular weight starch chains formed on radiation induced degradation, which are easier to disperse.[13,14,16–18,44–49] As discussed in the next section, degradation pattern of soil buried LT_{50} samples also indirectly indicate fine dispersal of starch phase in LDPE phase, but still the bond morphology is not co-continuous.

Surface wettability studies of composites

From the studies described in earlier sections, it was clear that dose imparted to RTPS significantly affects the morphology and biodegradation of the blends. To get a further understanding of the morphological and radiological changes taking place in the LDPE/RTPS blends, surface wet ability of different blends was investigated by contact angle measurement. The photographs recorded immediately after drops of water were allowed to fall on blends showed that initial contact angle decreased with increase in dose imparted to starch in LDPE/RTDS blend. This observation indicated (i) that either more RTPS moves to surface of the blends as the radiation dose increased (ii) if RTPS content remained the same the irradiation increased the wet ability of the blends surfaces. The kinetics of change in contact angle of the blends was also investigated and no significant change in kinetics was observed. To quantify the change in hydrophilic character of LDPE on introduction of RTPS surface energy of the blends of different composition was estimated. Water and diiodomethane were used as test liquids for determination of surface energy of the samples. Table VI gives the surface energy estimated for different samples. It is clear from the values in Table VI that irradiation of starch does increase the total surface energy of the blends to some extent but the increase in surface energy is not solely due to polar component, there is a proportionate increase in dispersive component as well. This indicates that not only polarity induced in the starch matrix (postulated due to generation of carbonyl and other groups) causes change in surface energy but also the morphological changes caused due to mixing also contribute to increase in surface energy. This was supported by the observations in the case of blends containing RTPS irradiated to higher radiation dose. The blends containing RTPS irradiated to higher radiation dose not only showed better uniform morphology but also further increase in both the components of surface energy.

Biodegradation behavior

The biodegradation behavior of the blends was monitored by placing the sample under subsoil condition for 3 months.[1,4,50] The weight loss of the samples (minimum five readings taken) was monitored and results of these studies are shown in Figure 7. The biodegradability of the blends was found to decrease with increase in the dose imparted to starch in RTPS. The weight loss of blend samples is solely due to removal of starch phase from the blends. Therefore, it can be concluded that 72–50% of the starch fraction biodegraded after 3 months of soil

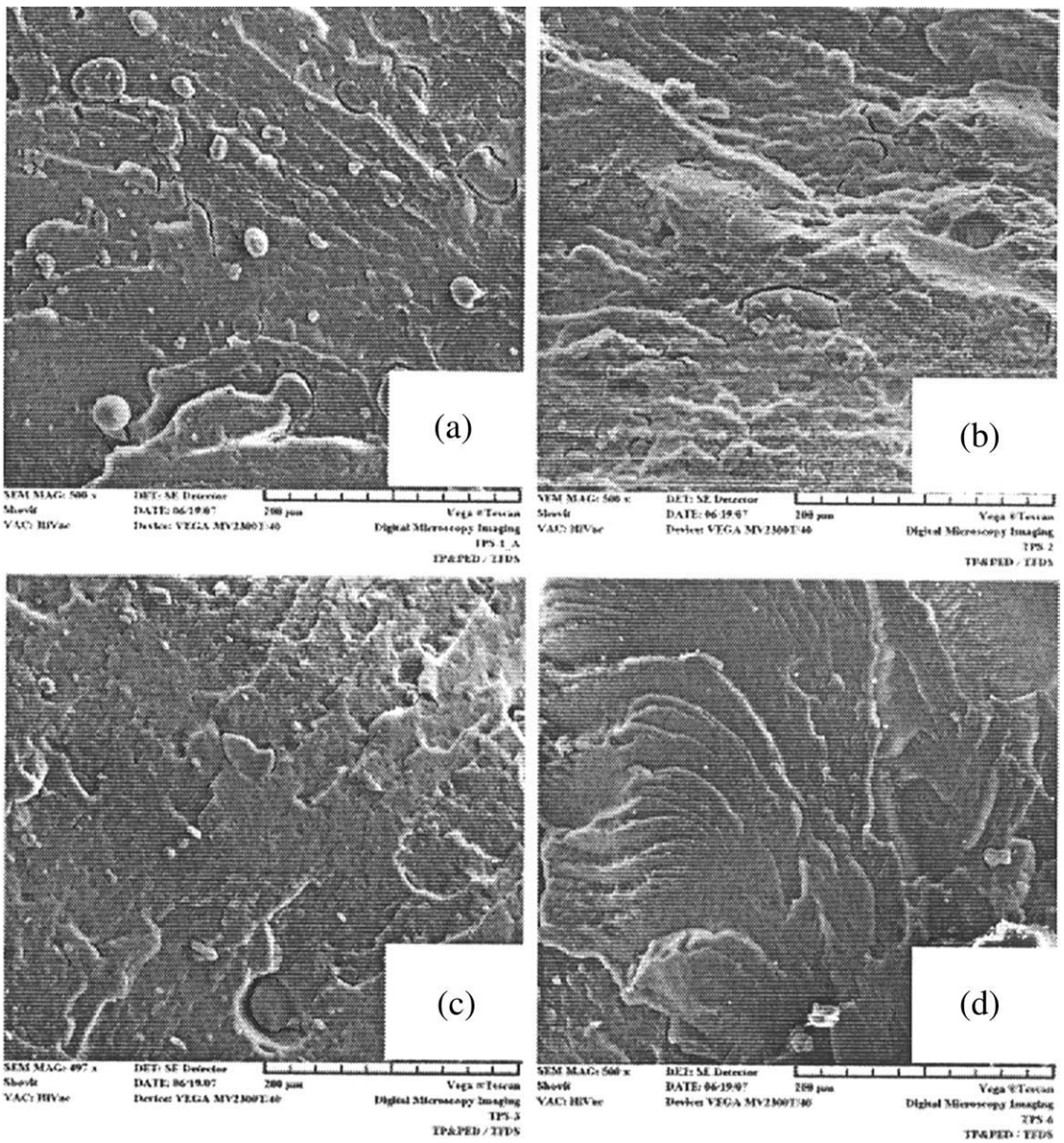

Figure 6 Scanning electron micrographs of LDPE/RTPS blends (a) LT_0, (b) LT_{10}, (c) LT_{25}, and (d) LT_{50}.

burial. Peanasky et al.[50] have established that percolation threshold for starch LDPE system is 0.3117 by volume. However, the high biodegradation of the LDPE/RTPS system suggests that mechanism of microbial invasion in raw starch and RTPS is different.

TABLE VI
Surface Energy of TPS Blends

	Surface energy (mJ/m^2)		
Sample	Total energy	Polar component	Dispersive component
LT_0	30.4	1.9	28.5
LT_{05}	34.4	2.8	31.7
LT_{10}	34.9	2.9	32.0
LT_{25}	34.9	3.8	31.0
LT_{50}	37.8	4.2	33.6

This can be primarily attributed to the difference in the compatibility and distribution of raw starch, TPS, and RTPS in LDPE. The overall increase in crystallinity of LDPE/RTPS (discussed earlier in "Thermal behavior of LDPE/TPS blend" Section) with increase in dose imparted to RTPS may also hinder the microbial damage to the blend matrix at the interphase. The FTIR-ATR spectrum of biodegraded LDPE/RTPS blends are shown in Figure 8. It is evident that peak due to O—H stretching (3000–3600 cm^{-1}) is not at all seen in subsoil conditioned blends whereas peaks in range 960–1200 cm^{-1} (attributed to C—O stretching of starch) could still be seen. This indicates that for starch the main chain degradation by cleavage of α-1-4 glycoside linkage is followed by selective removal of hydroxyl group

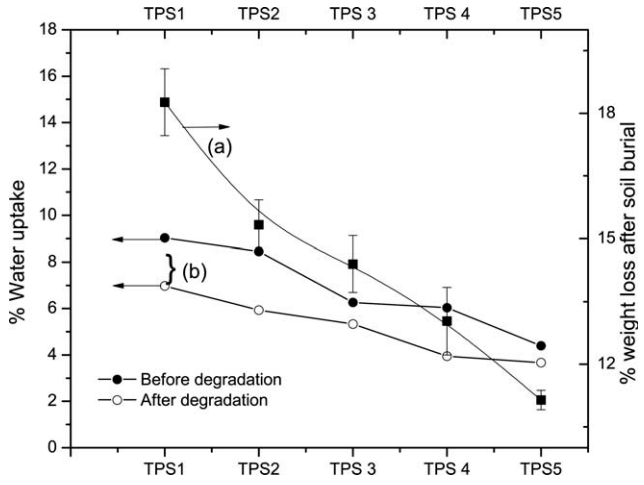

Figure 7 (a) Weight loss after 3 months of soil burial and (b) percentage water uptake of pristine and biodegraded LDPE/RTPS blends.

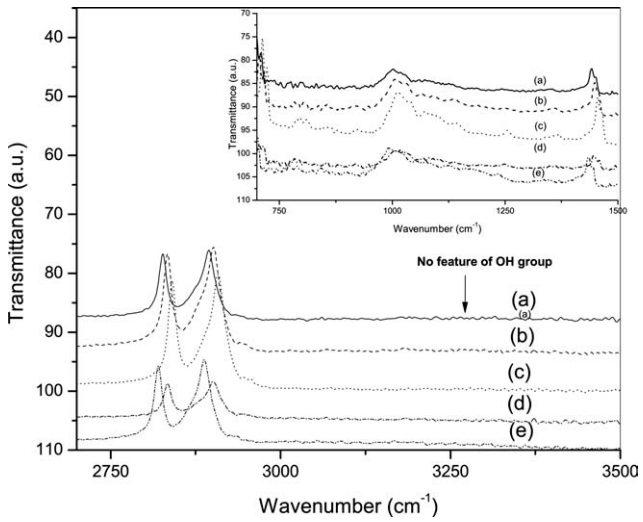

Figure 8 FTIR spectrum of biodegraded LDPE/RTPS blends (a) LT_0, (b) LT_5, (c) LT_{10}, (d) LT_{25}, and (e) LT_{50} at higher wave number. Inset: FTIR spectrum of biodegraded LDPE/RTPS blends at lower wave number.

and opening of ring is the last step in degradation of starch. Figure 7 shows water uptake of virgin and biodegraded LDPE/TPS blends. It is interesting to see that water uptake by the biodegraded blends ranging 7–4% even after 70–50% removal of starch, that is, it is not in linear proportion to residual starch in the biodegradable blends. Disproportionate water uptake may be assigned to the formation of microvoids and capillaries in the biodegraded blend matrix, which may eventually lead to an increase in the oxidative degradation of LDPE matrix. The optical micrographs of the biodegraded blends have been shown in Figure 9. As expected no damage was observed to pure LDPE film, however, blends containing different types of RTPS showed different topologies. Samples containing unirradiated starch showed maximum damage, and through holes were observed only for LT_0, which is in agreement with biodegradability results. LT_5 also showed severe damage and large zones due to starch removal; however, no through holes were detected. LT_{10} and LT_{25} showed relatively less damage whereas LT_{50} showed quite distinct pattern, exhibiting homogeneously dispersed starch domains which were considerably smaller than those of other blends. It was interesting to observe that though LT_{50} showed homogeneous

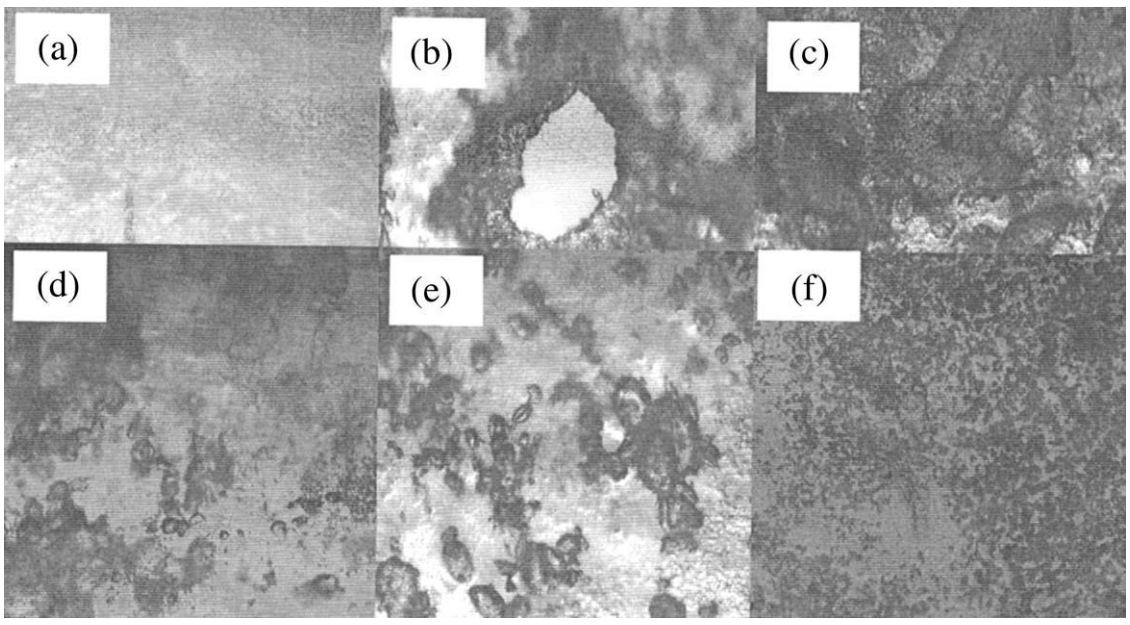

Figure 9 Optical micrographs (100×) of biodegraded LDPE/RTPS blends (a) pure LDPE, (b) LT_0, (c) LT_5, (d) LT_{10}, (e) LT_{25}, and (f) LT_{50}.

film structure, but it did not show continuous blend structure which could provide channels for microbial invasion. The decrease in the biodegradability of LT_{50} could therefore be attributed to the poor connectivity among starch layers and shielding of starch domains by LDPE.

CONCLUSION

The molecular weight of the starch reduces substantially after radiation treatment. The thermoplasticized lower molecular weight starch shows better miscibility with LDPE and changes morphology of the blends. This change in morphology has been primarily attributed to the kinetic factors affecting the phase separation of the blend components. The use of RTPS leads to improved processability of the blends and makes the processes less energy intensive. The study provides evidences of homogenization of blend morphology of LDPE/TPS blends when RTPS was used in preparation of blends. The DSC and XRD studies both suggested that an increase in the crystallinity of the LDPE phase with the use of radiation degraded starch, which was attributed to the relatively lesser hindrance by low molecular weight starch molecules to the crystallization of LDPE after melt mixing. No significant change in the carbonyl index was observed in the dose range of this study, therefore, change in the physical thermal properties was attributed primarily to entropic factors. Thermal degradation of the components in LDPE/RTPS was largely unaffected by radiation treatment. Both polar and dispersive components of surface energy increased for blends. Biodegradation of LDPE/RTPS was inhibited with increase in the dose imparted to starch, which has been attributed to poor connectivity of starch domain in LDPE phase as well as to the increased crystallinity of the LDPE domain when RTPS is used.

References

1. Chandra, R.; Rustgi, R. Prog Polym Sci 1998, 23, 1273.
2. Biresaw, G.; Mohamed, A.; Gordon, S. H.; Harry-O'kuru, R. E.; Carriere, C. C. J Appl Polym Sci 2008, 110, 2932.
3. González-Gutiérrez, J.; Partal, P.; García-Morales, M.; Gallegos, C. Carbohydr Polym 2011, 84, 308.
4. Steinbüchel, A. Curr Opin Biotechnol 1992, 3, 291.
5. Senna, M. M. H. Mater Res Innov 2005, 9, 84.
6. Willett, J. L. J. Appl Polym Sci 1994, 54, 1685.
7. Gupta, A. P.; Kumar, V.; Sharma, M. J Polym Environ 2010, 18, 484.
8. Krawczak, P. Exp Polym Lett 2008, 2, 237.
9. Ruiz, H. V.; Martínez, E. S. M.; Méndez, M. A. A. Starch-Starke 2011, 63, 42.
10. Bhandari, P. N.; Singhal, R. S. Carbohydr Polym 2002, 48, 233.
11. Bagheri, R. Radiat Phys Chem 2009, 78, 765.
12. Mishra, S.; Bajpai, R.; Katare, R.; Bajpai, A. K. Exp Polym Lett 2007, 1, 407.
13. Henry, F.; Costa, L. C.; Aymes-Chodur, C. Radiat Phys Chem 2010, 79, 75.
14. Kamal, H.; Sabry, G. M.; Lotfy, S.; Abdallah, N. M.; Ulanski, P.; Rosiak, J.; Hegazy, E. S. A. J Macromol Sci Pure 2007, 44, 865.
15. Kong, X.; Kasapis, S.; Bao, J.; Corke, H. Radiat Phys Chem 2009, 78, 954.
16. Sagar, A. D.; Villar, M. A.; Thomas, E. L.; Armstrong, R. C.; Merrill, E. W. J Appl Polym Sci 1996, 61, 139.
17. Sagar, A. D.; Villar, M. A.; Thomas, E. L.; Armstrong, R. C.; Merrill, E. W. J Appl Polym Sci 1996, 61, 157.
18. Senna, M. M.; Yossef, A. M.; Hossam, F. M.; El-Naggar, A. W. M. J Appl Polym Sci 2007, 106, 3273.
19. Dubey, K. A.; Pujari, P. K.; Ramnani, S. P.; Kadam, R. M.;Sabharwal S. Radiat Phys Chem 2004, 69, 395.
20. Ershov, B. G.; Klimentov, A. S. Russ Chem Rev 1984, 53, 1195.
21. Charlesby, A. Radiat Phys Chem 1977, 9, 17.
22. Dubey, K. A.; Bhardwaj, Y. K.; Chaudhari, C. V.; Bhattacharya, S.; Gupta, S. K.; Sabharwal, S. J Polym Sci Polym Phys 2006, 44, 1676.
23. Chaudhary, A. L.; Torley, P. J.; Halley, P. J.; McCaffery, N.; Chaudhary, D. S. Carbohydr Polym 2009, 78, 917.
24. Kurata, M.; Tsunashima, Y.; Iwama, M.; Kamada, K. In Polymer Handbook, 4th ed.; Brandrup, J.; Immergut, E.H., Eds.; Wiley-Interscience: New York, 1975; p 45.
25. Gao, J.; Wang, D.; Yu, M.; Yao, Z. J Appl Polym Sci 2004, 93, 1203.
26. Loo, Y. L.; Wakabayashi, K.; Huang, Y. E. Polymer 2005, 46, 5118.
27. Erbil, H. Y. In Handbook of Surface and Colloid Chemistry; Birdi, K. S., Ed.; CRC Press: Boca Raton, New York, 1997, p 265.
28. Hoover, R.; Sosulski, F. Starch-Stärke 1985, 37, 181.
29. Yang, J. H.; Yu, J. G.; Ma, X. F. Carbohydr Polym 2006, 66, 110.
30. Pedroso, A. G.; Rosa, D. Carbohydr Polym 2005, 59, 1.
31. Tena-Salcido, C.; Rodríguez-González, F.; Méndez-Hernández, M.; Contreras-Esquivel, J. Polym Bull 2008, 60, 677.
32. Albertsson, A. C.; Griffin, G. J. L.; Karlsson, S.; Nishimoto, K.; Watanabe, Y. Polym Degrad Stab 1994, 45, 173.
33. Bikiaris, D.; Panayiotou, C. J Appl Polym Sci 1998, 70, 1503.
34. Ferreira, F. G. D.; de Andrade Lima, M. A. G.; de Almeida, Y. M. B.; Vinhas, G. M. J Polym Environ 2010, 18, 196.
35. Ghosh, R. N.; Jana, T.; Ray, B. C.; Adhikari, B. Polym Int 2004, 53, 339.
36. Rubens, P.; Heremans, K. Biopolymers 2000, 54, 524.
37. Li, C.; Kong, Q.; Zhao, J.; Zhao, D.; Fan, Q.; Xia, Y. Mater Lett 2004, 58, 3613.
38. Vega, D.; Villar, M. A.; Failla, M. D.; Vallés, E. M. Polym Bull 1996, 37, 229.
39. Rodriguez-Gonzalez, F. J.; Ramsay, B. A.; Favis, B. D. Polymer 2003, 44, 1517.
40. Yoda, O.; Tamura, N.; Doi, K. J Mater Sci 1976, 11, 696.
41. Alexander, L. E. X-ray Diffraction Methods in Polymer Science; Wiley-Interscience: New York, 1969.
42. Hofmann, D.; Fink, H. P.; Philipp, B. Polymer 1989, 30, 237.
43. Kresge, E. N. Rubber Chem Technol 1991, 64, 469.
44. Abu, J. O.; Minnaar, A. Int J Food Sci Technol 2009, 44, 2335.
45. Ibrahim, S. M. J Appl Polym Sci 2011, 119, 685.
46. Rahmat, A. R.; Rahman, W. A.; Sin, L. T.; Yussuf, A. A. Mater Sci Eng 2009, 29, 2370.
47. Senna, M. M.; Hossam, F. M.; El-Naggar, A. W. M. Polym Compos 2008, 29, 1137.
48. Singh, S.; Singh, N.; Ezekiel, R.; Kaur, A. Carbohydr Polym 2011, 83, 1521.
49. Yu, Y. F.; Cui, J.; Chen, W. J.; Li, S. J. J Macromol Sci Pure 1998, 35, 121.
50. Peanasky, J. S. Long, J. M.; Wool, R. P. J Polym Sci Pol Phys 1991, 29, 565.